

Optimum tailor-welded blank design using deformation path length of boundary nodes

Ali Fazli¹

1. Assistant Professor, Mechanical Engineering Department, Faculty of Engineering and Technology, Imam Khomeini International University, Qazvin, Iran

a.fazli@ikiu.ac.ir

Abstract

In this paper, the optimum shape of Tailor-Welded Blanks (TWB) is investigated. The optimization is performed for two different case studies. The first example is deep drawing of a TWB with dissimilar materials and uniform thicknesses and the next example is deep drawing of a TWB with similar materials and non-uniform thicknesses. The effect of blank optimization on the weld line movement is investigated. Also the effect of weld line location on the blank optimization and weld line movement is examined.

Keywords: Deep drawing; Blank shape optimization; Tailor-welded blanks; Weld line location; Weld line movement

1. INTRODUCTION

A Tailor-Welded Blank (TWB) consists of sheet metals with similar/dissimilar and uniform/non-uniform thicknesses welded together to produce a single blank prior to the forming process. In order to reduce vehicle weight and manufacturing costs, application of the TWBs in the automotive industries have increased recently. However, it is important to understand and predict the parameters influencing the deep drawing of TWBs.

Some of the characteristics of the deep drawing of TWBs have been studied and reported in the literature. Heo et al. [1] investigated the weld line movement in deep drawing of laser welded blanks. They also studied the effects of the drawbead dimension on the weld line movement in the deep drawing process [2]. He et al. [3] proposed a strategy to control the weld line movement, using the control of the blankholder force. Bravar et al. [4] predicted the initial weld line placement using an analytical model and compared the results with the numerical simulations. Padmanabhan et al. [5] studied the effect of the anisotropy of the blank sheets in deep drawing of TWBs. Tang et al. [6] developed a one-step finite element code InverStamp which can be used to design TWBs, predict the movement of the weld line and optimize the position of the weld line. Rojek et al. [7] presented some experimental and experimental-numerical methods which can be used to determine mechanical properties of the weld zone in tailor-

welded blanks. Padmanabhan et al. used the numerical simulations to determine the stress states and their influence on the springback behavior of deep-drawn tailor-welded blanks [8]. Valente et al. [9] investigates the influence of different finite element formulations in the performance and quality of solution obtained by numerical simulation in the analysis of tailor-welded hydroformed tubular parts. Abbasi et al. [10] analyzed the wall wrinkling tendency of a TWB, analytically, numerically and experimentally.

Among all the process parameters in deep drawing of TWBs, its optimum shape is one of the important factors, because it minimizes the forming defects, improves the formability of the sheet metal, the quality and thickness distribution of the drawn cup and also reduces the material cost. Therefore the design of the optimum TWB is a vital desire of the industries.

Several methods have been developed for the optimum blank design. Kuwabara and Si [11] designed the optimum blank using the slip-line field theory. The method is capable of predicting an optimal blank shape within few seconds but assumes the blank material as isotropic, rigid perfectly plastic. The change of the blank thickness during deep drawing process is neglected. Kim and Kobayashi [12] designed the blank shape of rectangular cups by proposing a velocity field with some assumed parameters in the deformation domain. The values of the assumed parameters are determined using experiments. Zaky et al. [13] used the stress and strain

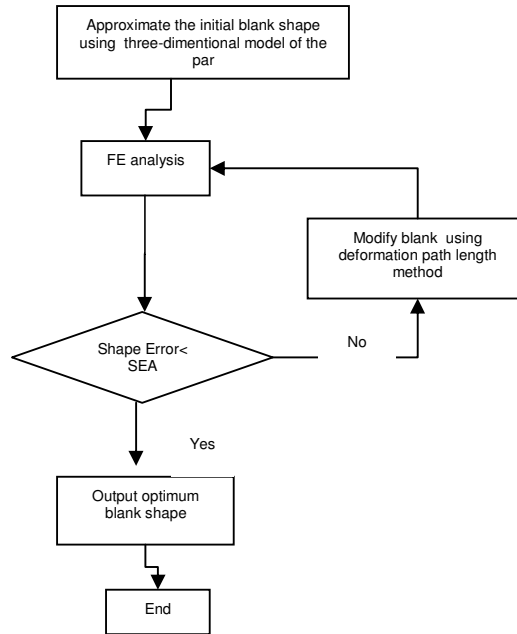


Fig1. Blank optimization procedure presented by Fazli and Arezoo [23]

Relationship according to the Hill's theory to calculate the optimum blank shape of cylindrical cups in the deep drawing of anisotropic sheet metals. Batoz et al. [14] proposed an inverse finite element method (IFEM) to obtain the initial blank shape and the thickness strain distribution by assuming membrane stress and total deformation theory of plasticity. Guo et al. [15] derived a nonlinear formulation for the field problems as an inverse method to obtain the initial blank shape and the strain distribution in a deformed part. Parsa and Pournia [16] developed the optimum blank with IFEM and compared it with conventional forward incremental. Azizi and Assempour [17] developed a linear IFEM to design the optimum blank. Kim et al. [18] proposed a roll-back method to predict the optimum initial blank shape in the sheet metal forming processes and applied it to design the weld line in a tailor-welded blank. Shim and Son [19] proposed the sensitivity method where an initial blank is supplied and the position of the point on the initial contour is modified iteratively by measuring the shape error with the known final cup shape. Son and Shim [20] proposed a method that iteratively designs the optimum blank shape using the initial nodal velocity of the boundary nodes. Vafaeseefat used the iteration of FE simulation

to optimize the initial blank shape [21]. His blank modification algorithm is based on the projection of the target contour on the deformed blank and modifying the blank shape accordingly. Hammami et al. [22] developed the push/pull optimization technique to design the optimum blank. Fazli and Arezoo [23] approximated an initial blank geometry using the three-dimensional geometry of the given part and optimized this blank iteratively based on the shape error and the deformation path length of the boundary nodes. They also compared their algorithm with some other iteration based algorithms and found their algorithm to be more efficient [24]. De-Carvalho et al. [25] presented an optimization procedure to define the initial geometry of a sheet metal blank to produce a uniform thickness final part. Ku et al. [26] applied the backward tracing scheme for the rigid-plastic finite element method to design the initial tailor-welded blank for net-shape production and verified it by a rectangular example.

Although the optimum blank shape design for traditional blanks are reported in the literature, according to the knowledge of the author, except the work of Ku et al. [26], no rigorous attempt was made to predict the optimum shape of the tailor-welded blanks.

In this study, the approach developed by Fazli and Arezoo [23] for optimum blank design is applied to the TWBs and the results are investigated. Primarily an initial blank is designed using the three-dimensional geometry of the given product. The forming process is numerically simulated using this initial blank. The blank is iteratively optimized based on the shape error and the deformation path length of the boundary nodes of the previous deformed blank. The effect of some process parameters on the optimum blank shape is examined. During simulation, the difference between the material properties of Heat-Affected Zone (HAZ) and the base materials is neglected, since the width of the weld line and HAZ is relatively small in comparison to the overall size of the blank [26].

2. The blank optimization procedure

The flow chart of the blank optimization presented by Fazli and Arezoo [23] is shown in Figure 1. Primarily, the initial blank is approximated using the three-dimensional geometry of given product. The forming process is simulated using this initial blank. The deformed edge contour of the blank is compared with the target edge contour of the product geometry. If the shape error (which is the distance of the boundary nodes to the target edge contour in direction of the deformation path) is larger than the predefined value of Shape Error Allowance (SEA), the blank is modified using the developed algorithm and the forming process is simulated again. This process is repeated until the shape error is less than the predefined value of SEA at every boundary node. The

initial blank approximation and the blank optimization algorithm are described in [23].

2. Examples

In order to examine the optimization method on the tailor-welded blanks, the optimization is performed for two different case studies. The first case study is deep drawing of a TWB made of dissimilar materials and uniform thicknesses and the next example is deep drawing of a TWB made of similar materials and non-uniform thicknesses. The deformation process is simulated using the finite element software ABAQUS/Explicit. The blank is modeled with a four-node linear shell element (S4R) and the tools are created using the rigid elements (R3D4).

3.1. Deep drawing of TWBs with dissimilar materials

The first case study is a deep drawn cup with a square cross section, made of two dissimilar materials DP600 and DC06 and uniform thicknesses. The drawing depth is 40mm and the geometry of drawing tools and desired part shape are shown in Figure 2 the properties of materials are given in Table 1. The left side of the TWB is considered from the weaker material DC06 and the right side of the TWB is considered from the stronger material DP600. The optimum blank shapes are obtained for five different Weld Line Location (WLL) of the sheet metals, which it is considered to be located at 0, 12, 24, -12 and -24mm from the centerline of the drawing dies.

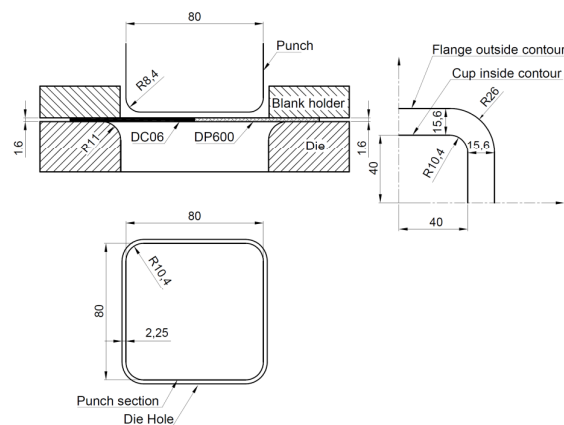


Fig2. Forming tool geometry for square cup drawing with dissimilar materials and the desired part shape

Table: Materials properties for FE simulation of square cup drawing with dissimilar material

Material	DC06	DP600
Young modulus E(GPa)	210	210
Poisson's ratio, ν	0.3	0.3
Anisotropy ratios	r_0	2.53
	r_{90}	2.72
	r_{45}	1.84
Yield Stress, σ_y (MPa)	123.6	330.3
Stress Constant, K(MPa)	529.5	1093
strain hardening exponent, n	0.268	0.187
Coefficient of frictions, μ	0.1	0.1
Sheet metal thickness, mm	1.6	1.6

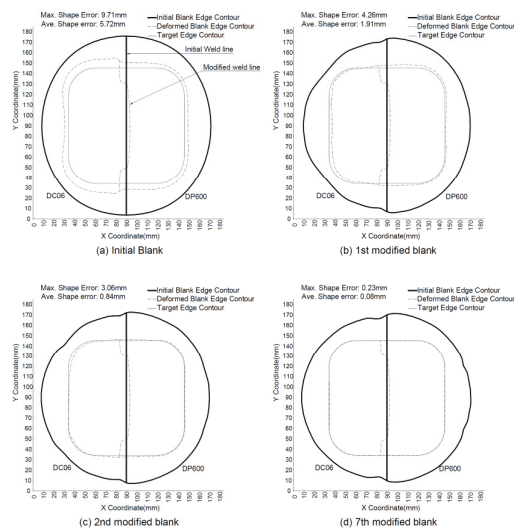
**Fig3.** Evaluation of flange edge and weld line contour after deformation for tailor-welded square cup with two different materials a) initial blank b) 1st modified blank c) 2nd modified blank d) 7th modified blank

Figure 3 shows the blank edge contour, the drawn cup edge contour and the target edge contour for the initial blank, first, second and seventh modified blanks respectively for the condition where the weld line is located at the centerline of the drawing die (WLL=0mm). Also the maximum shape error and average shape error for each drawn blank are

represented in this figure. It can be seen that the shape error decreases in each modification compared to previous blank and it is reduced from 9.71mm in initial blank to 0.23mm in 7th modified blank. So the path length method is successful in prediction of optimum blank shape for tailor-welded blanks. The

deformed shape of the initial and optimum blanks for $WLL=0\text{mm}$ are shown in Figure 4.

Figure 5. Shows the weld line movement for the initial and optimum blanks for the condition where WLL is 0mm . It can be seen that for both initial and optimum blanks, in the bottom of drawn cup, the weld line moves from the weaker material (DC06) toward the stronger material (DP600), while in the flange of the drawn cup, the weld line moves from the stronger material toward the weaker material. Also it can be seen that the weld line movement in the optimum blank is slightly less than in the initial blank, both in the bottom and the flange of the drawn cup. So the blank optimization decreases the weld line movement.

The blank optimization is performed for various

WLL and the maximum shape errors for all iterations of optimization are shown in Figure 6. As it is shown, the convergence of the blank optimization is related to the position of the weld line. It can be seen that the maximum shape error converges when WLL is 0mm , 12mm and -12mm , while it does not converge when WLL is -24mm and 24mm . When WLL is 0mm , the maximum shape error converges to smaller values and it oscillates about the value 0.4mm , while when it is 12mm and -12mm , the maximum shape error oscillates about the values of 0.8mm and 1.2mm , respectively. So the convergence of the maximum shape error is completely related to the WLL and it may not converge when the WLL is far from the centerline of the drawing tools.

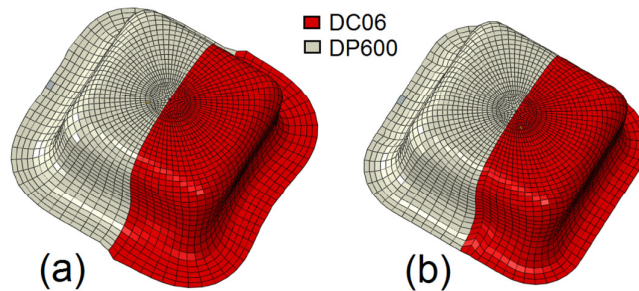


Fig4. The deformed shape of the TWBs for $WLL=0\text{mm}$. a) initial blank. b) optimum blank.

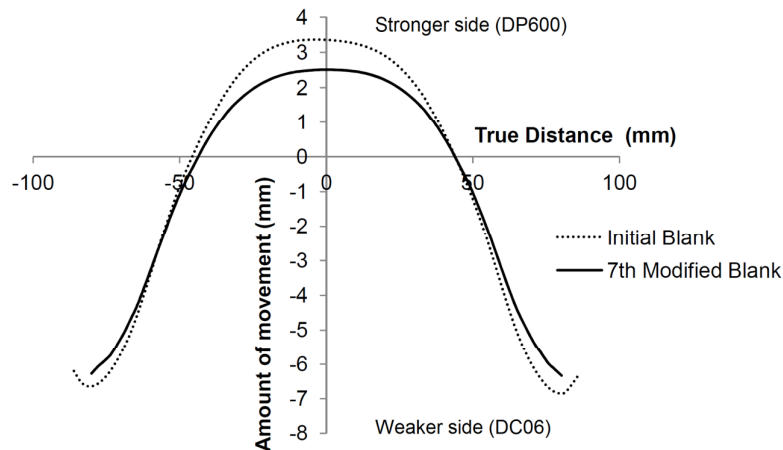


Fig5. Weld line movement in the initial and optimum blank for $WLL=0\text{mm}$

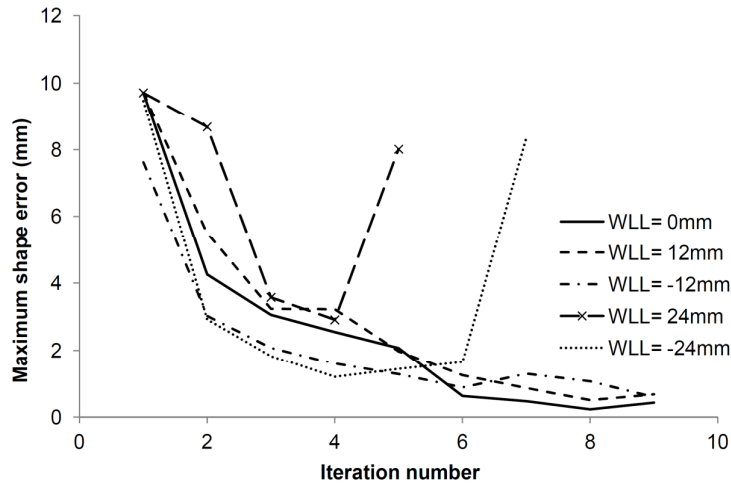


Fig6. Comparison of maximum shape error obtained in all iterations of various WLL.

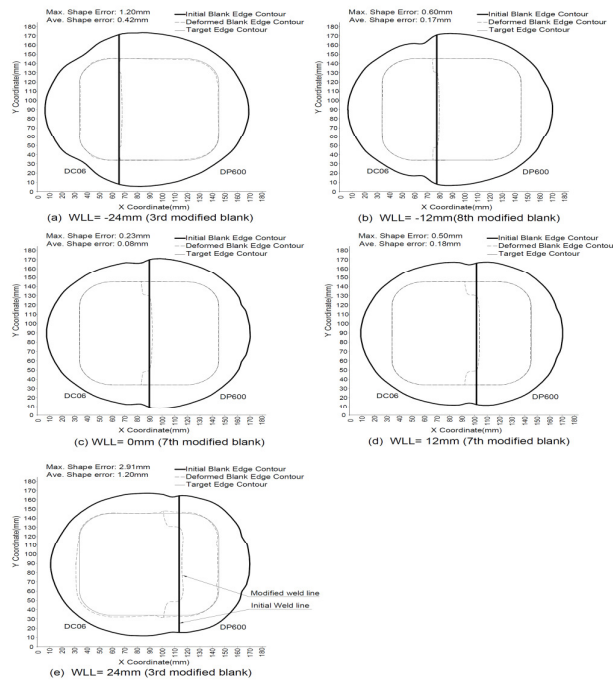


Fig7. Comparison of optimum blanks shape for various WLL. a) WLL=-24mm b)WLL=-12mm c)WLL=0mm d)WLL=12mm e)WLL=24mm

The optimum blank shape for various WLL is shown in Figure 7. It can be seen that optimum blank shapes for various WLL are not the same and it is affected by the position of the weld line.

The weld line movement for each WLL is shown in Figure 8. As shown in this figure, for all WLL, in the bottom of drawn cup, the weld line moves from the weaker material (DC06) toward the stronger material (DP600), while in the flange of the drawn

cup, the weld line moves from the stronger material toward the weaker material. However, it can be seen that the weld line movement at the bottom of the cups are almost the same for all WLL, while the weld line movement at the flange of the drawn cup is considerably related to WLL. The maximum weld line movement in the flange is for WLL=24mm

where most of the blank is made from the weaker material and its minimum movement is for WLL=-24mm where most of the blank is made from the stronger material. This effect can also be seen in Figure 7.

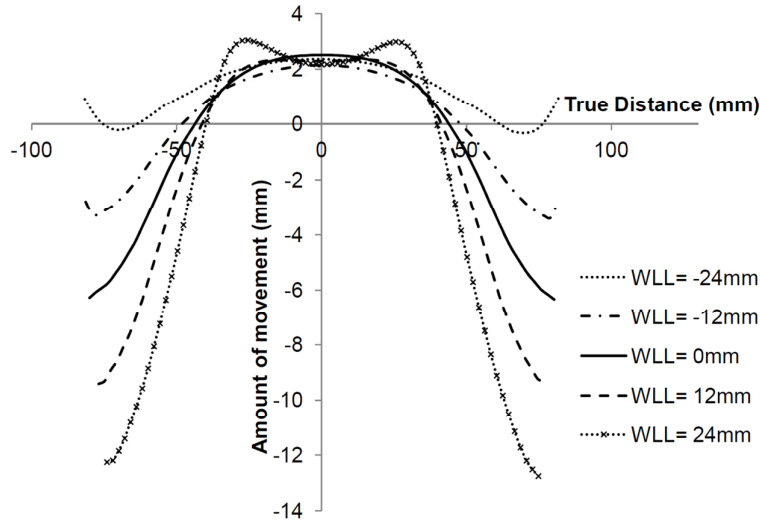


Fig8. Comparison of the weld line movement of the optimum blanks in various WLL.

Table 2- Materials properties for FE simulation of square cup drawing with similar materials and non-uniform thickness

Young modulus E(GPa)		210
Poisson's ratio, ν		0.3
Anisotropy ratios	r_0	1.0
	r_{90}	1.0
	r_{45}	1.0
Yield Stress, σ_y (MPa)		137
Stress Constant, K(MPa)		498
strain hardening exponent, n		0.21
Coefficient of frictions, μ		0.1

3.2. Deep drawing of TWBs with non-uniform thickness

The second case study is the same as the previous square cup, but it is made of sheet metals with non-uniform thicknesses of 1.6mm and 0.8mm and similar material SPC1. The material properties of drawn cup are given in Table 2. The drawing depth is 40mm and

the geometry of the drawing tools are shown in Figure 9. The left side of the TWB has a thickness of 1.6mm, while the right side of the TWB has a thickness of 0.8mm. The same as previous case study, the optimum blank shapes are obtained for five different WLL, where it is considered to be located at 0, 12, 24, -12 and -24mm from the centerline of the drawing dies. The punch, the die and the blank holder have modeled to have a step to consider the thickness difference of the two sides. However, since during the deep drawing of the TWB, the weld line moves, so the die should be made such that the thicker side never contacts the step. Therefore, as shown in Figure 9, the tools step is offset 5mm toward the thinner side. When the weld line movement is more than 5mm, the offset is increased.

The blank optimization of TWBs with similar materials and non-uniform thicknesses is performed for various WLL and the maximum shape error for all iterations of optimization, is shown in Figure 10. As it can be seen, the convergence of the blank optimization is related to the position of the weld line. It can be seen that the maximum shape error converges when WLL is 0mm, 12mm and -12mm and -24mm, while it does not converge when WLL is 24mm. It can be seen that, when the weld line location is closer to the centerline of the drawing die, the blank optimization converges to a smaller values of shape error and when the WLL is far from the centerline of the drawing tools, the blank optimization may not converge.

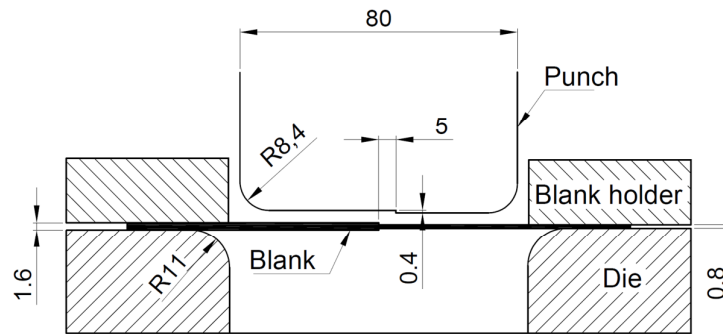


Fig9. Forming tool geometry for drawing TWB with similar materials and non-uniform thickness.

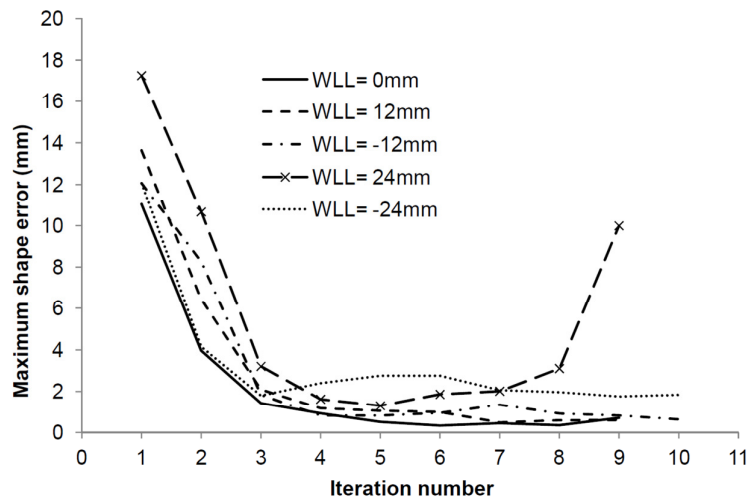


Fig10. Comparison of maximum shape error obtained in all iterations of various WLL.

The optimum blank shape is shown in Figure 11 for various WLL. It can be seen that optimum blank

shape for various WLL are not the same and it is affected by the position of the weld line.

The weld line movement of TWBs with non-uniform thickness is shown in Figure 12 for each WLL. As it can be seen, for all WLL, in the bottom of the drawn cup, the weld line moves from the thinner side (THK=0.8mm) toward the thicker side (THK=1.6mm). In the flange of the drawn cup, for all cases except WLL=24mm, the weld line moves from the thicker side toward the thinner side. The

maximum weld line movement in the bottom and flange of the drawn cup is when WLL= -24mm i.e. when most of the blank is made of the thinner sheet metal, while minimum weld line movement in the bottom and flange of the drawn cup is when WLL= 24mm i.e. when most of the blank is made of the thicker sheet metal. This effect can also be seen in Figure 11.

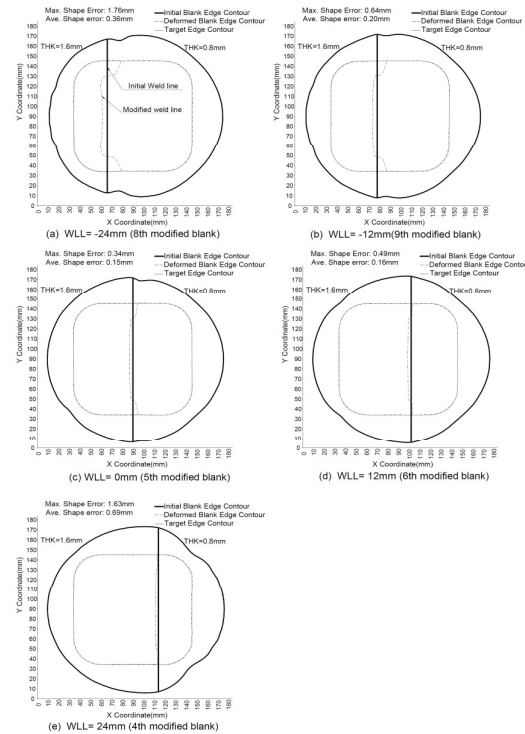


Fig11. Comparison of optimum blanks shape for various WLL. a) WLL=-24mm b)WLL=-12mm c)WLL=0mm d)WLL=12mm e)WLL=24mm

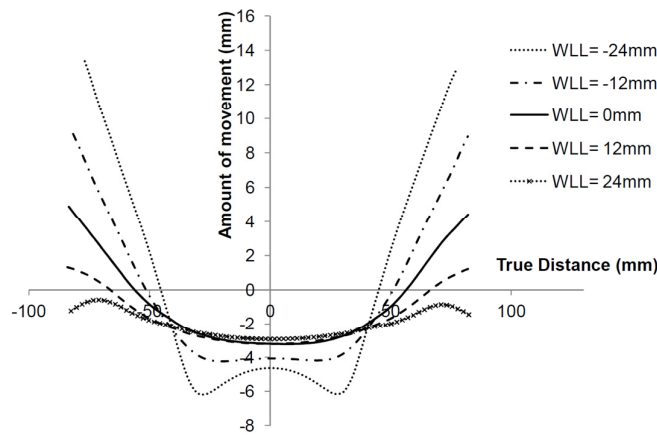


Fig12. Comparison of the weld line movement of the optimum blanks in various WLL.

Conclusion

In the present work the optimum blank shape for Tailor-Welded Blanks (TWB) are determined. Using the three-dimensional geometry of the given product, an initial blank is approximated and the forming process is simulation using this blank. The initial blank is iteratively optimized based on the distance of the boundary nodes to the target edge contour. The optimum blank shape is obtained for a TWB with dissimilar materials and uniform thicknesses and also for a TWB with similar materials and non-uniform thicknesses. It can be concluded from the present work that:

- The weld line location affects the optimum blank shape of TWB.
- The blank optimization reduces the weld line movement.
- When the weld line location (WLL) is on the centerline of the drawing die, the optimization converges to the smaller shape errors, while when the WLL is not on the centerline, it converges to the larger shape errors. When the WLL is far from the centerline, the blank optimization may not converge.
- In deep drawing of TWB with dissimilar materials and uniform thicknesses, when most of the blank is made of the weaker material the weld line movement is maximum and when most of the blank is made of the stronger material, the weld line movement is minimum.
- In deep drawing of TWB with similar materials and non-uniform thicknesses, when most of the blank is made of the thinner sheet metal, the weld line movement is maximum and when most of the blank is made of the thicker sheet metal, the weld line movement is minimum.

References

- [1]. Heo YM, Kim HY, Seo D, Choi Y (2000) Investigations of weld-line movements for the deep drawing process of tailor welded blanks. *J Mater Process Technol* 108:1-7
- [2]. Heo YM, Wang SH, et al (2001) The effect of the drawbead dimensions on the weld-line movements in the deep drawing of tailor-welded blanks. *J Mater Process Technol* 113: 686–691
- [3]. He S, Wu X, Hu SJ (2003) Formability enhancement for tailor-welded blanks using blank holding force control. *J Manuf Sci Eng: Trans ASME* 125:461–467
- [4]. Bravar MN, Kinsey BL (2004) Analytical determination of initial weld lineposition for tailor welded blank forming. *Trans North Am Manuf Res Inst SME* 32: 597–604
- [5]. Padmanabhan R, Baptista AJ, Oliveira MC, Menezes LF (2007) Effect ofanisotropy on the deep-drawing of mild steel and dual-phase steel tailor-weldedblanks. *J Mater Process Technol* 184: 288–293
- [6]. Tang BT, Zhao Z, Yu S, Chen J, Ruan XY (2007) One-step FEM based control of weld line movement for tailor-welded blanks forming. *J Mater Process Technol* 187–188: 383–386
- [7]. Rojek J, Hycza-Michalska M, Bokota A, Piekarska W (2012) Determination of mechanical properties of the weld zone in tailor-welded blanks. *Archives of Civil and Mech Eng* 12:156–162
- [8]. Padmanabhan R, Oliveira MC, Laurent H, Alves JL, Menezes LF (2009) Study on springback in deep drawn tailor welded blanks. *Int J Mater Form* 2:829-832
- [9]. Valente RAF, Alves de Sousa RJ, Natal Jorge RM (2009) Enhanced finite element formulations on the numerical simulation of tailor-welded hydroformed products. *Int J Mater Form* 2:927-929
- [10]. Abbasi M, Ketabchi M, Labudde T, Prah U, Bleck W (2012) New attempt to wrinkling behavior analysis of tailor welded blanks during the deep drawing process. *Mater Des* 40:407–414
- [11]. Kuwabara T, Si WH (1997) PC-based blank design system for deep-drawing irregularly shaped prismatic shells with arbitrarily shape flange. *J Mater Process Technol* 63:89–94
- [12]. Kim N, Kobayashi S (1986) Blank design in rectangular cup drawing by an approximate method. *Int J Mach Tool Des Res* 26:125–135
- [13]. Zaky AM, Nassr AB, El-Sebaie MG (1998) Optimum blank shape of cylindrical cups in deep drawing of anisotropic sheet metal. *J Mater Process Technol* 76:203–211
- [14]. Batoz JL, Guo YQ, Detraux JM (1990) An inverse finite element procedure to estimate the large plastic strain in sheet metal forming. In: Third international conference on technology of plasticity, Kyoto 1403–1408
- [15]. Guo YQ, Batoz JL, Naceur H, Bouabdallah S, Mercier F, Barlet O (2000) Recent developments on the analysis and optimum design of sheet metalforming parts using a simplified inverse approach. *Comput Struct* 78:133-148

- [17]. Parsa MH, Pournia P (2007) Optimization of initial blank shape predicted based on inverse finite element method. *Finite Elem Anal Des* 43:218–233
- [18]. Azizi R, Assempour A (2008) Applications of linear inverse finite element method in prediction of the optimum blank in sheet metal forming. *Mater Des* 29:1965-1972
- [19]. Kim JY, Kim N, Huh MS (2000) Optimum blank design of an automobile sub-frame. *J Mater Process Technol* 101:31–43
- [20]. Shim H, Son K (2002) Optimal blank shape design by the iterative sensitivity method. *Proc IMechE Part B: J Engineering Manufacture* 216:867–878
- [21]. Son KC, Shim HB (2003) Optimal blank shape design using the initial velocity of boundary nodes. *J Mater Process Technol* 134:92–98
- [22]. Vafaesehat A (2008) Optimum blank shape design in sheet metal forming by boundary projection method. *Int J Mater Form* 1:189-192
- [23]. Hammami W, Padmanabhan R, Oliveira MC, BelHadjSalah H, Alves JL
- [24]. and Menezes LF (2009) A deformation based blank design method for formed parts. *Int J Mech Mater Des* 5:303–314
- [25]. Fazli A, Arezoo B (2012) Optimum blank shape design using shape error and deformation path length of boundary nodes. *Proc IMechE Part B: J Engineering Manufacture* 226:684-693
- [26]. Fazli A, Arezoo B (2012) A comparison of numerical iteration based algorithms in blank optimization. *Finite Elem Anal Des* 50:207-216
- [27]. De-Carvalho R, Silva S, Valente RAF, Andrade-Campos A (2012) Blank optimization in a stamping process-Influence of the geometry definition. *Finite Elem Anal Des* 61:75-84
- [28]. Ku TW, Kang BS, Park HJ (2005) Tailored blank design and prediction of weld line movement using the backward tracing scheme of finite element method. *Int J Adv Manuf Technol* 25:17–25